ARCHIVES OF ACOUSTIC
4, 3 (1979)

INVESTIGATION OF THE ACOUSTIC FIELD DISTRIBUTION IN PIEZOELECTRIC TRANSDUCERS BY THE BRAGG DIFFRACTION METHOD

ZYGMUNT KLESZCZEWSKI

Institute of Physics of Silesian Technical University (44-100 Gliwice)

In the paper the possibility of using the light, diffracted by acoustic waves, for the investigation of the distribution of acoustic fields in solids is presented, and the results obtained are described. Quartz and $LiIO_3$ transducers with a fundamental frequency of 200-400 MHz were the sources of a longitudinal acoustic wave. The transducer length was several mm, and the transducer width was about 1 mm. Fused and crystalline quartzes were used as media. The acoustic field was probed with a narrow laser beam, and the angular distribution of the diffracted light intensity was measured. The experimental results obtained were compared with theoretical calculations.

1. Introduction

One of possible uses of the interaction of an acoustic wave and a laser beam is the determination of the intensity distribution in acoustic fields in solids.

In practical applications transducers of very small dimensions (2-5 mm²) are very often used, particularly for frequencies above 100 MHz. The application of a laser beam to investigate such transducers is very useful because it can be narrowly collimated. At the same time, the knowledge of the acoustic beam geometry in such transducers is sometimes very important, particularly in acousto-optical devices. The investigation of the field distribution by the Bragg diffraction method is performed by the measurement of the diffracted light intensity distributions or, as mentioned above, by probing the field with a suitably narrow laser beam [2, 4, 6].

The objectives of this paper are a brief theoretical discussion of the problem and a description of the experimental results obtained.

2. Theoretical basis. Angular distribution of the diffracted light intensity

Let us assume that an acoustic wave with a frequency Ω and a wave vector $\boldsymbol{q}$ propagates in a medium (Fig. 1). Its passage causes a change in the electrical permeability of the medium,

$$\varepsilon = \varepsilon^{(0)} + \Delta\varepsilon(y)\sin(qz - \Omega t), \tag{1}$$

where $\varepsilon^{(0)}$ is the electrical permeability of the undisturbed medium, and $\Delta\varepsilon(y)$ – the electrical permeability variation amplitude.

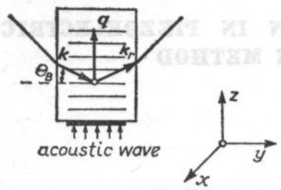

Fig. 1. The Bragg diffraction geometry
$\boldsymbol{k}$ – the incident light wave vector, $\boldsymbol{k}_r$ – the undulatory light vector after diffraction, $\boldsymbol{q}$ – the undulatory vector of the light wave

If a laser beam also travels in the medium, then for the geometry shown in Fig. 1 the electrical field intensity of the light wave may be expressed in the form

$$E_0 = V_0 \exp\{i(ky\sin\theta - kz\cos\theta - \omega t)\}, \tag{2}$$

where V_0, k, ω are the amplitude, wave vector and frequency of the incident light wave, respectively.

In the present case of light diffraction by acoustic waves of high frequency (above 200 MHz), only lines of the first order appear in the spectrum of the diffracted light. Thus, the electrical field of the diffracted light wave may be expressed in the form

$$\begin{aligned} E_1 = {} & V_1(y)\exp\{i[ky\sin\theta + (k\cos\theta + q)z - (\omega + \Omega)t]\} + \\ & + V_{-1}(y)\exp\{i[k\sin\theta + (k\cos\theta - q)z - (\omega + \Omega)t]\}, \end{aligned} \tag{3}$$

where $V_1(y)$ and $V_{-1}(y)$ are the amplitudes of the diffracted light wave for the first order lines.

Using the wave equation

$$\nabla^2 \boldsymbol{E} = \frac{1}{c^2}\frac{\partial^2}{\partial t^2}(\varepsilon \boldsymbol{E}) \tag{4}$$

and equations (1)-(3), one can show [8] that the diffracted light amplitude may be expressed by the formula

$$V_1 = e^{-i\beta y}\int_{y_1}^{y_2} \alpha V_0 e^{i\beta y'}\,dy', \tag{5}$$

where

$$\alpha = \frac{\Delta\varepsilon(y)k}{4\varepsilon\cos\theta}, \quad \beta = \frac{q}{\cos\theta}(\sin\theta_B - \sin\theta),$$

and θ_B is the Bragg angle.

The integration limits are defined by the area of the interaction of the light and acoustic waves. An analogous equation can be obtained for the line of order -1.

A practical calculation of V_1 from equation (5) requires a knowledge of $\Delta\varepsilon(y)$. We shall consider the simplest cases of the relation $\Delta\varepsilon(y)$, assuming at the same time that the variation in the electrical permeability of the medium is proportional to the acoustic wave amplitude.

1. $a = a_0$ in the area $-L/2 \leqslant y \leqslant L/2$ (a flat transducer with a uniform amplitude distribution).

Then from formula (5) we have

$$\frac{V_1}{V_0} = a_0 L e^{iqy\Delta\theta} \frac{\sin(qL\Delta\theta/2)}{qL\Delta\theta/2}, \tag{6a}$$

$$\frac{I_1}{I_0} = \left|\frac{V_1}{V_0}\right|^2 = a_0^2 L^2 \frac{\sin^2(qL\Delta\theta/2)}{(qL\Delta\theta/2)^2}, \tag{6b}$$

where I_1/I_0 is the ratio of the diffracted and the incident light intensities.

Furthermore, if $\theta = \theta_B$ and the diffracted light intensity is small, the ratio I_1/I_0 is proportional to the acoustic beam intensity [8].

2. $a = a_0 e^{-y^2/R^2}$. We have

$$\frac{V_1}{V_0} = e^{-iqy\Delta\theta} \sqrt{\pi} a_0 R e^{-(q\Delta\theta R)^2/4}, \tag{7a}$$

while

$$\frac{I_1}{I_0} = \left|\frac{V_1}{V_0}\right|^2 = \pi a_0^2 R^2 e^{-(q\Delta\theta R)^2/2}. \tag{7b}$$

3. If

$$a = \begin{cases} a_0 & \text{for } -\tfrac{1}{2}(W+L) \leqslant y \leqslant -\tfrac{1}{2}(W-L) \\ & \text{and } \tfrac{1}{2}(W-L) \leqslant y \leqslant \tfrac{1}{2}(W+L), \\ 0 & \text{outside this area,} \end{cases}$$

then

$$\frac{V_1}{V_0} = -2a_0 L e^{iqL\Delta\theta} \frac{\sin(qL\Delta\theta/2)}{qL\Delta\theta/2} \cos\frac{qW\Delta\theta}{2}, \tag{8a}$$

$$\frac{I_1}{I_0} = 4a_0 L^2 \frac{\sin^2(qL\Delta\theta/2)}{(qL\Delta\theta/2)^2} \cos^2\frac{qW\Delta\theta}{2}. \tag{8b}$$

It follows from (6)-(8) that the ratio V_1/V_0 is the Fourier transform of the function a. From measurements of the angular distribution of the diffracted light intensity, we can draw conclusions about the vibration amplitude distribution on the transducer surface. It should be stressed, however, that the measurement of I_1/I_0 gives only the ratio $|V_1/V_0|$ and that the calculation of the inverse Fourier transform from the experimental curve is quite complicated. In the experimental part we shall show that, however, these measurements give much information about the transducer oscillations.

3. Acoustic field in flat and cylindrical transducers

In addition to the angular distributions discussed above, application of Bragg diffraction permits the acoustic field to be probed with a suitably narrow laser beam. From these measurements it is possible to determine directly the relative intensity of the acoustic field in a crystal, at the point of the interaction of the acoustic wave and light.

The acoustic field amplitude at any point of the field can be calculated, using the well-known [7] diffraction formula

$$S(x, y, z) = \frac{iq}{2\pi}\int_A\int S(x_0, y_0, 0)\frac{|z|}{r^2}e^{-iqr}dx_0 dy_0, \quad (9)$$

where $S(x_0, y_0, 0)$ is the vibration amplitude and (x_0, y_0) are the coordinates of a point in the plane of the transducer.

For an anisotropic medium the case is more complicated because the velocity of acoustic wave propagation is different in different crystallographic directions. This is accounted for numerically by the so-called *anisotropy parameter* expressed by the elastic constants of shape. A detailed discussion of the problem for an anisotropic medium can be found in paper [1].

Figure 2 shows the position of the transducer in the coordinate system assumed for the calculations. The transducer dimensions and the direction of the laser light propagation are also marked there. In the measurement

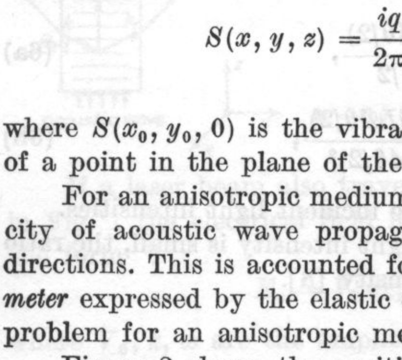

Fig. 2. Transducer dimensions and position in the coordinate system assumed for calculation

method, used for the results reported here, the laser beam interacted with the acoustic wave along the whole cross-section of the ultrasonic wave. Therefore, an additional integration along the direction Y should be carried out in expression (9) (Fig. 2). In consequence, taking into account the elastic anisotropy of the medium and the attenuation of the acoustic wave, for the acoustic field amplitude $S(x, z)$, related to the total path of the interaction of the light and the acoustic wave, we get

$$S(x,z) = \frac{iqe^{-\alpha z}}{2\pi(1-2b)} \int\limits_{-\infty}^{\infty} \int\limits_{-d/2}^{d/2} \int\limits_{-d'/2}^{d'/2} S(x_0, y_0, 0) \times \\ \times \exp\left\{iq\left[z + \frac{(x-x_0)^2+(y-y_0)^2}{2z(1-2b)}\right]\right\} dy dx_0 dy_0, \quad (10)$$

where a is the attenuation coefficient for the acoustic wave and b — the anisotropy parameter.

Values of the anisotropy parameter for some crystallographic systems are given in paper [5]. For the present case of the acoustic wave propagation along the Z axis of crystals of the trigonal system we have

$$b = \frac{(C_{33}-C_{13}-2C_{44})(C_{33}+C_{13})}{2C_{33}(C_{33}-C_{44})}, \quad (11)$$

where C_{ij} are components of the tensor of elastic constants.

If a flat transducer with a uniform amplitude distribution is the source of the field, then

$$S(x_0, y_0, 0) = \begin{cases} S_0 & \text{for } -\frac{d}{z} \leqslant x_0 \leqslant \frac{d}{2} \text{ and } -\frac{d'}{z} \leqslant y_0 \leqslant \frac{d'}{2}, \\ 0 & \text{outside this area.} \end{cases} \quad (12)$$

Substituting (12) into (10), after an elementary integration we obtain

$$|S(x,z)|^2 = S_0^2 e^{-2\alpha z} \frac{d'^2}{\Lambda z(1-2b)} \left| \int\limits_{-d/2}^{d/2} \exp\left\{-iq\frac{(x-x_0)^2}{2z(1-2b)}\right\} dx_0 \right|^2, \quad (13)$$

where Λ is the acoustic wavelength.

The field intensity distribution according to (13) was calculated, using a digital computer. Figure 3 shows an example of the theoretical intensity distribution of an acoustic field at a frequency of 215 MHz in crystalline quartz for a propagation direction along the Z axis. It was assumed that $d' = 5$ mm, $d = 1$ mm, and that the parameter b — calculated from expression (11) — is in the present equal to -0.232.

If, however, a cylindrical transducer with a uniform amplitude distribution is the source of the field, then

$$S(x_0, y_0, 0) = \begin{cases} S_0 e^{iqx_0^2/2R} & \text{for } -\frac{d}{2} \leqslant x_0 \leqslant \frac{d}{2} \text{ and } -\frac{d'}{2} \leqslant y_0 \leqslant \frac{d'}{2}, \\ 0 & \text{outside this area.} \end{cases} \quad (14)$$

Substituting (14) into (10) we obtain

$$|S(x,z)|^2 = \\ S_0^2 e^{-2\alpha z} \frac{d'^2}{\Lambda z(1-2b)} \left| \int\limits_{-d/2}^{d/2} \exp\left\{\frac{iqxx_0}{z(1-2b)} + \frac{iqx_0^2}{2}\left[\frac{1}{R} - \frac{1}{z(1-2b)}\right]\right\} dx_0 \right|^2. \quad (15)$$

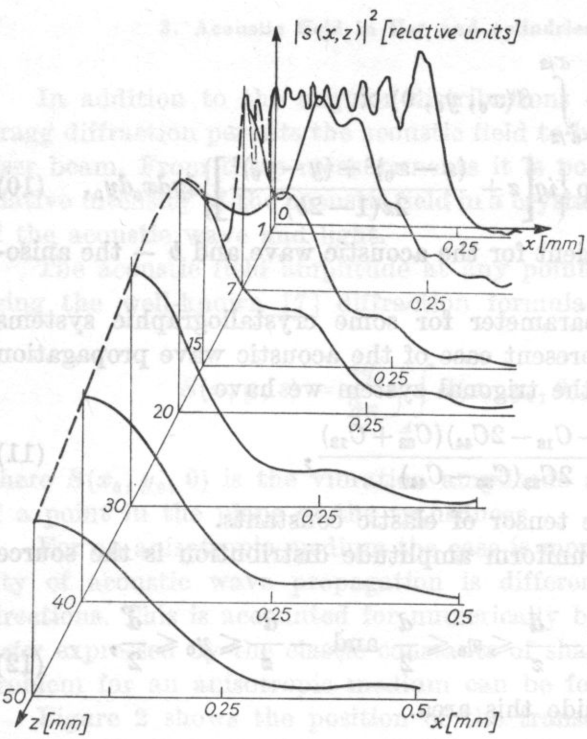

Fig. 3. Theoretical distribution of the acoustic field intensity produced by a flat transducer
$f = 216$ Hz, $d' = 5$ mm, $d = 1$ mm, $b = -0.232$

The results of measurements of the field intensity distribution at a frequency of 340 MHz are presented in Fig. 4. It has been assumed that $R = 5$ mm, $d = 4$ mm, $d' = 6$ mm, $b = -0.232$. It should be noted that the distance from the acoustic beam focus in anisotropic media is different from R, and is $R' = R/(1-2b)$. In the present case $R' = 3.41$ mm.

4. Measurement system

The measurement system used is shown in Fig. 5. Quartz and $LiIO_3$ transducers working at fundamental frequencies between 200-400 MHz were the sources of longitudinal acoustic waves. The transducers were excited form generators $G3$-20 and $G4$-37A, modulated by rectangular pulses with a duration of 0.1 μs and a repetition frequency of 1 kHz. Crystals, in which the distributions of acoustic fields were investigated, had lengths from 40 to 60 mm and transverse dimensions 10×10 mm. In the investigation of the distribution of acoustic fields, created by flat transducers, the back wall of the crystal was ground at an angle of several degrees to the acoustic wave front. This prevented diffraction of light by the reflected wave or the occurrence of a stationary wave. In the investigation of the acoustic field distribution of the focussed diffracted wave, however, the back wall of the crystal had

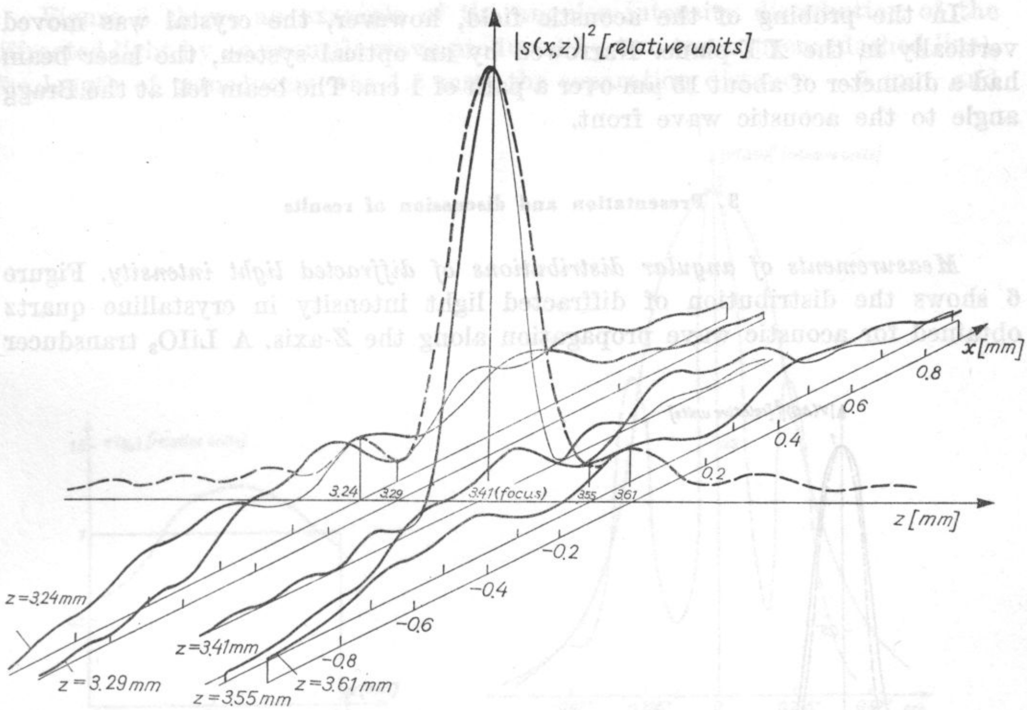

Fig. 4. Theoretical distribution of the acoustic field produced by a cylindrical transducer $f = 340$ MHz, $d' = 6$ mm, $d = 4$ mm, $R = 5$ mm, $b = -0.232$, $R' = R/(1-2b) = 3.41$ mm

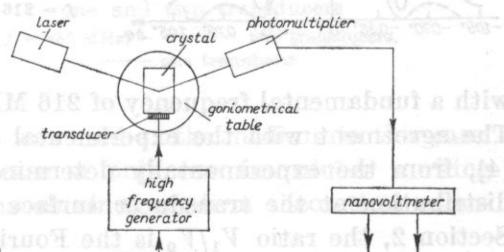

Fig. 5. Block diagram of the experimental apparatus

a cylindrical surface, the passage time of the acoustic wave was considerably longer than the duration of the acoustic pulse but at the same time considerably shorter than the pulse repetition time. The crystals were placed on a goniometrical table, which ensured precise turning and moving of the sample.

A 5-mW He-Ne laser was the light source. Diffracted light was registered by a photomultiplier from which a signal was shown on nanovoltmeter and a pen recorder.

Angular distributions of the diffracted light intensity were measured with the crystal being rotated in the diffraction plane. The angle $\Delta\theta$ was measured with an accuracy of 1′.

In the probing of the acoustic field, however, the crystal was moved vertically in the XY-plane. Narrowed by an optical system, the laser beam had a diameter of about 15 μm over a path of 1 cm. The beam fell at the Bragg angle to the acoustic wave front.

5. Presentation and discussion of results

Measurements of angular distributions of diffracted light intensity. Figure 6 shows the distribution of diffracted light intensity in crystalline quartz obtained for acoustic wave propagation along the Z-axis. A $LiIO_3$ transducer

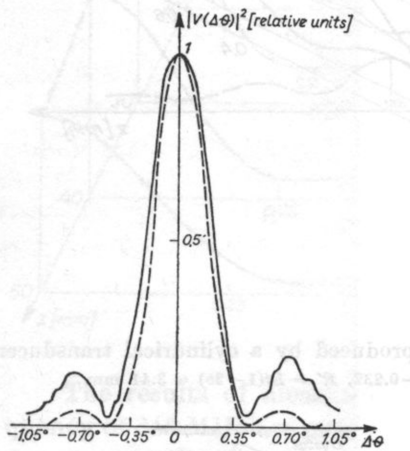

Fig. 6. Angular distribution of the diffracted light intensity in crystalline quartz

f = 216 MHz,——— experimental curve, – – – – – theoretical curve

with a fundamental frequency of 216 MHz was the source of the acoustic wave. The agreement with the experimental curve is not very good. Using relation (4), from the experimentally determined behaviour of $I(\Delta\theta)$, the amplitude distribution at the transducer surface was estimated. As was mentioned in Section 2, the ratio V_1/V_0 is the Fourier transform of the function $a(y)$. Calculating the inverse Fourier transform, we obtain $a(y)$ if we know $|V_1/V_0|$.

It should be noted, however, that we obtain only V_1/V_0 measurements and we do not know the analytical form of the relation $V_1\Delta\theta/V_0$. Therefore, to calculate the inverse transform we used the trapezoidal method of approximation. The results of the calculation are shown in Fig. 7 (for one half of the transducer). The dashed line shows the vibration amplitude distribution at the transducer, obtained by the method discussed, while the full line represents the vibration amplitude distribution on an ideal transducer. The experimentally obtained distribution differs from the uniform distribution assumed.

It appears that the above method, although it is approximate and slightly troublesome in calculation, can be successfully used for determination of the vibration amplitude in piezoelectric transducers.

Figure 8 shows an example of the angular intensity distribution of the diffracted light by an acoustic wave produced by two transducers (dashed line). The length of transducers was 1.5 mm, the separation distance – 5 mm, and

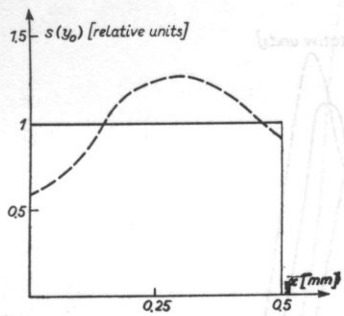

Fig. 7. Vibration amplitude on the transducer surface studied

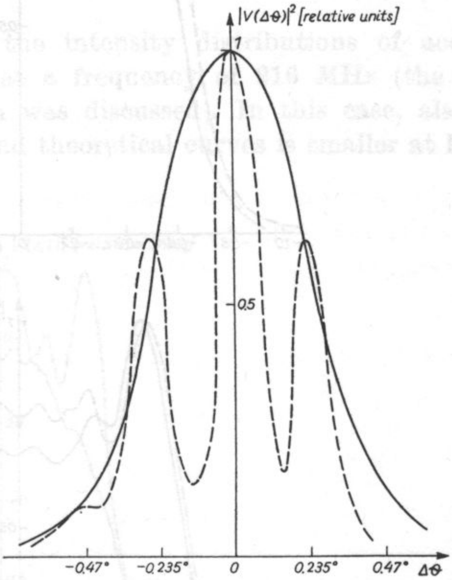

Fig. 8. Angular distribution of the acoustic field intensity produced by one and two transducers

f = 285 MHz, – – – – – two transducers, ——— one transducer

the frequency – 285 MHz. Fused quartz was used as the medium in this case. For comparison, the behaviour in the case of only one transducer working (full line) is also presented. The relations obtained confirm theoretical calculations performed in point two.

Acoustic field probing. In the measurements performed, attention was paid to direct measurement of the acoustic field intensity and the effect of focussing on the field distribution. The measurements were made by probing the acoustic field with a laser beam. The measurements were restricted to the Fresnel zone which in the present case was several centimetres long.

Figs. 9a, 9b and 9c show the intensity distributions of acoustic fields in the fused quartz obtained at distances of 2, 3 and 7 mm from a $LiIO_3$ transducer whose dimensions were $d' = 8$ mm, $d = 1.5$ mm, and whose frequency was 200 MHz. It follows from a comparison of the experimental and theoretical behaviour that the agreement is not very good close to the transducer, while further away the experimental and theoretical behaviours were practically the same. It seems that the fact that it does not vibrate in a piston mode, which

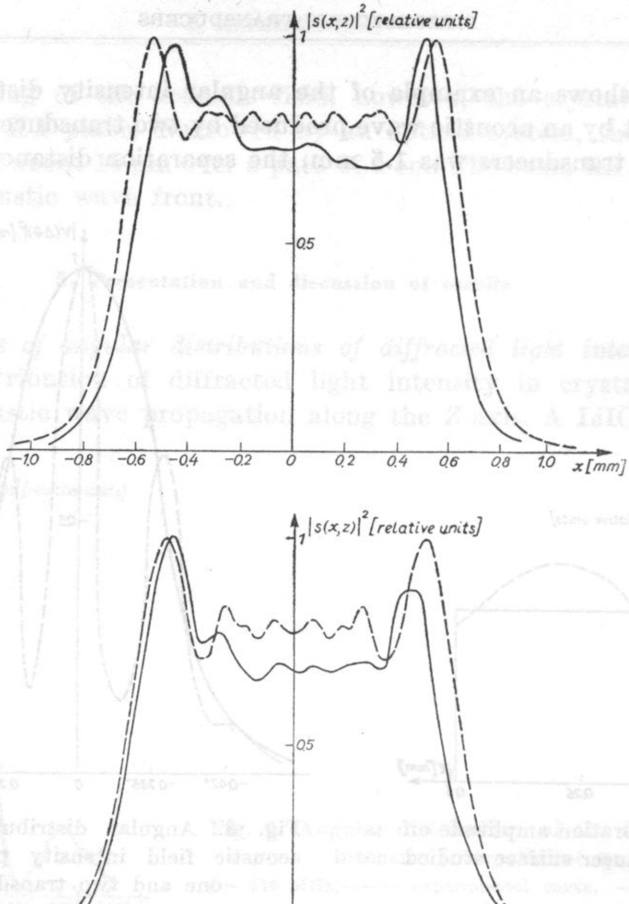

Fig. 9. Distribution of the acoustic field intensity in fused quartz at various distances from the transducer

f = 200 MHz, d' = 8 mm, d = 1.5 mm, (a) z = 2 mm, (b) z = 3 mm, (c) z = 7 mm, ——— experimental curve, - - - - - theoretical curve

was also shown by measurement of angular distributions, is the main reason for this difference close to the transducer. Inadequate narrowing of the laser beam had a great effect on the results obtained.

It is difficult, however, to obtain a narrowing to several μm over a path of 1 cm.

Figures 10a and 10b represent the intensity distributions of acoustic fields in crystalline quartz obtained at a frequency of 216 MHz (the same transducer whose angular distribution was discussed). In this case, also the difference between the experimental and theoretical curves is smaller at longer distances from the transducer.

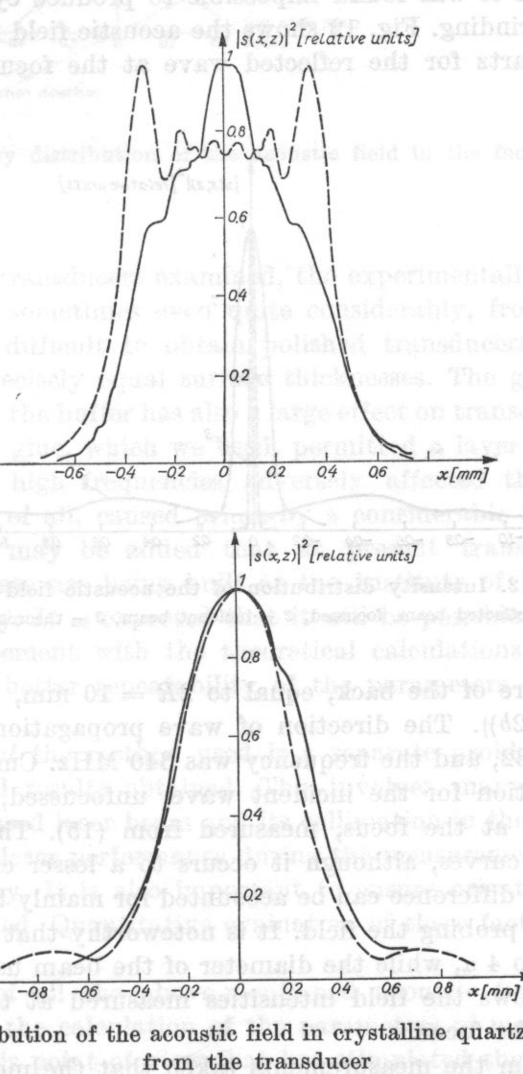

Fig. 10. Intensity distribution of the acoustic field in crystalline quartz at various distances from the transducer

$f = 216$ MHz, $d' = 5$ mm, $d = 1.5$ mm, (a) $z = 2$ mm, (b) $z = 15$ mm, ——— experimental curve, – – – – – theoretical curve

The investigation of focussing was performed in the system shown in Fig. 11. The reflection of the acoustic beam from the back, cylindrical wall of the buffer was used here. The use of such an acoustic focussing mirror was

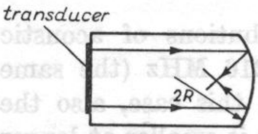

Fig. 11. Focussing acoustic mirror

necessary because it was found impossible to produce cylindrical transducers by the manual grinding. Fig. 12 shows the acoustic field intensity distribution in crystalline quartz for the reflected wave at the focus (curve *1*). For the

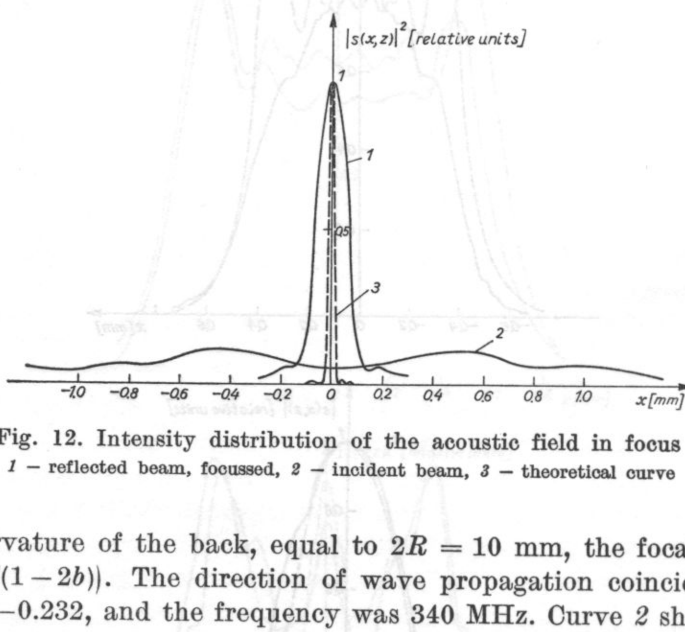

Fig. 12. Intensity distribution of the acoustic field in focus
1 — reflected beam, focussed, *2* — incident beam, *3* — theoretical curve

radius of curvature of the back, equal to $2R = 10$ mm, the focal length was 3.41 mm $(R/(1-2b))$. The direction of wave propagation coincided with the Z-axis, $b = -0.232$, and the frequency was 340 MHz. Curve *2* shows the field intensity distribution for the incident wave, unfocussed, and the theoretical field distribution at the focus, measured from (15). The focussing effect is distinct in these curves, although it occurs to a lesser extent than predicted theoretically. The difference can be accounted for mainly by the large diameter of the laser beam probing the field. It is noteworthy that theoretical focussing should occur up to 4 μ, while the diameter of the beam used was 15 μ.

Figure 13 shows the field intensities measured at the focus and 1 mm before and after the focus.

It follows from the measurements taken that the method can be successfully used for the investigation of acoustic field distributions in crystals.

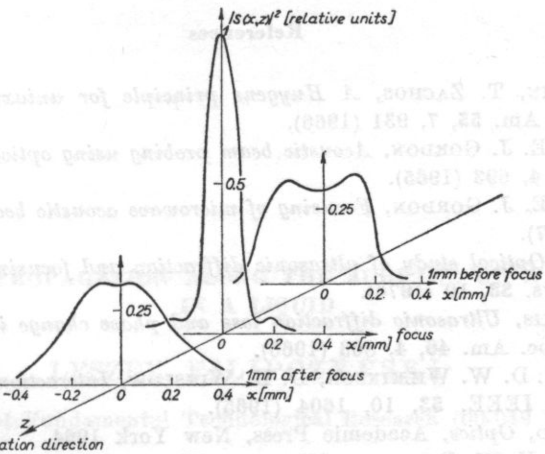

Fig. 13. Intensity distribution of the acoustic field in the focussing system

As regards the transducers examined, the experimentally determined field distribution differs, sometimes even quite considerably, from the theoretical distributions. It is difficult to obtain polished transducers with thicknesses of several μ and precisely equal surface thicknesses. The glue layer coupling the transducers with the buffer has also a large effect on transducer performance. The "Cyjanopan B" glue, which we used, permitted a layer of several μ to be obtained which at high frequencies adversely affected the transducer performance and, first of all, caused primarily a considerable loss in the electric power supplied. It may be added that at present transducers adhesively coupled with the base are being built at the Institute of Physics of Silesian Technical University. It is expected that it will be possible to obtain a considerably better agreement with the theoretical calculations with these transducers, and also a better repeatability of the parameters of the transducers made.

The precision of the method used is a separate problem in the analysis of the experimental results obtained. This involves many factors, e.g. the diameter of a narrowed laser beam and its collimation in the area investigated, the stability of the laser performance during the measurements, and the recording system stability. It is also important to ensure orientation precision for the samples examined. Quantitative evaluation of these factors is a very complicated matter.

A knowledge of all the above-mentioned acoustic field distributions is very important for the calculation of the parameters of many acousto-optical devices and it is this point of view that has stimulated the measurements described in this paper.

References

[1] L. Bergstein, T. Zachos, *A Huygens principle for uniaxially anisotropic media*, J. Opt. Soc. Am. **55**, 7, 931 (1966).

[2] M. G. Cohen, E. J. Gordon, *Acoustic beam probing using optical techniques*, Bell Syst. Tech. J. **44**, 4, 693 (1965).

[3] M. G. Cohen, E. J. Gordon, *Focusing of microwave acoustic beams*, J. Appl. Phys. **38**, 5, 2340 (1967).

[4] M. G. Cohen, *Optical study of ultrasonic diffraction and focusing in anisotropic media*, J. Appl. Phys. **38**, 10 (1976).

[5] E. P. Papadakis, *Ultrasonic diffraction loss and phase change in anisotropic materials*, J. Acoust. Soc. Am. **40**, 4, 863 (1966).

[6] G. F. Quate, C. D. W. Wilkinson, D. K. Winslow, *Interaction of light and microwave sound*, Proc. IEEE. **53**, 10, 1604 (1965).

[7] A. Sommerfeld, *Optics*, Academic Press, New York 1964.

[8] J. W. Tucker, V. W. Rampton, *Microwave Ultrasonics in Solid State Physics*, North-Holland Publishing Company, Amsterdam 1972.

Received on November 7, 1977;
final version — on January 10, 1979